DSS 14 64-Meter Antenna — Computed RF Pathlength Changes Under Gravity Loadings

M. S. Katow

DSN Engineering Section

Using a computer model of the reflector structure and its supporting assembly of the 64-m antenna rotating about the elevation axis, the radio frequency (RF) pathlengths changes resulting from gravity loadings were computed. A check on the computed values was made by comparing the computed foci offsets with actual field readings of the Z or axial focussing required for elevation angle changes.

I. Introduction

The Cassegrainian geometry of the radio frequency (RF) reflectives surfaces of the 64-m antenna is set or rigged to the design values at 45 degrees elevation angle. A change in the elevation angle then results in a gravity loading increment. This gravity loading deflects the parabolic reflector and the sub-reflector position and results in a change of the RF path distance from the target or RF source to the RF feed's phase center on the antenna.

Only the pathlength changes resulting from gravity loading are considered in this article. The very long baseline interfer-ometry (VLBI) target locating system may be affected by the RF path changes under all environmental loading conditions on the antenna. Reporting on wind loading effects on path changes will follow.

The distortion analyses were made using the NASTRAN structural computing program. The analytical model consisted of a half-symmetrical model using all of the stressed bars and plates of the reflector structure attached to its elevation wheel truss structure. All bars of the quadripod truss supporting the subreflector were also in the model.

II. Analysis Description

The RF optics system is illustrated in Fig. 1, where the equivalent zero gravity loading condition is at the rigging angle. At this elevation angle, the surface panels of the main reflector are set to the design paraboloid and the hyperboloid is aligned on the paraboloid's axis. When the elevation angle is changed from the rigging angle, the gravity loading resulting from the rotation of the gravity vector with respect to the symmetric axes of the antenna distorts the reflector structure. Its RF performance is then defined by best fitting a paraboloid to the displaced surface panel's supporting joints. The com-puted best fit paraboloid (Ref. 1) data are shown in Table 1 as changes from the rigging angle. Figure 2 illustrates the data along with the central ray starting from the virtual focus of the hyperboloid system and reflected from the vertex of the best fit paraboloid.

The manufactured and gravity distortions of the surface panels as well as the small gravity distortions of the hyperboloid's surface were considered to have negligible effect on RF path changes. The deflection of the hyperboloid's axis results in offsets at the primary focus from the RF feed and at the virtual secondary focus from the focus of the best fit paraboloid. These offsets will result in path length changes.

Figure 3 illustrates the central RF ray from the RF feed through the hyperboloid system and reflected from the vertex of the best fit paraboloid. The hyperboloid was simulated on the structural model by its vertex node 2093 and a node 2094 on axis. From the displacement output of these two nodes the positions of the hyperboloid's axis were calculated and noted in Table 2. The phase centers offsets were calculated and noted on Table 3 and illustrated in Fig. 3.

The RF pathlength changes were calculated by tracing the length changes of the central ray for two cases. For the first case (a), the hyperboloid was not controlled, which resulted in off Z focus operation of the paraboloid. In the second case (b), the hyperboloid was always moved in Z direction to the focussed position where the gain was maximized. For case (a), the pathlength changes are summarized in Table 4 and plotted in Fig. 4. For case (b), the pathlength changes are summarized in Table 5 and plotted in Fig. 4.

III. Field Check

A field check of the important computed numbers was available from the console indication of the hyperboloid's Z axis position as the Cassegrain system was maintained in focus through the elevation angle range. In Ref. 2, a record of the indicated control room position of the hyperboloid was kept for the focussed case with the antenna receiving at X- and K-band. The readout in the control room indicates only the Z extension or contraction of the jackscrews. Thus, corrections for the deflections of the jackscrews bolted on the apex of the

quadripod were made. The hyperboloid's system corrections were also made. Table 6 illustrates the field data corrected to output the Z foci offsets and plotted in Fig. 5. Also plotted are the computed Z offsets.

IV. Conclusions

(1) Although the "no Z focus curve" of Fig. 4 shows much smaller pathlength changes, there will be gain losses due to foci offsets at X-band operation which may result in signal deterioration or loss. Also, the computed central ray pathlength changes may not accurately reflect the pathlength changes of the actual completely integrated RF wave front when the paraboloid is operated off focus. Table 7 shows the gain losses at X-band (8.45 GHz) for the computed foci offsets.

(2) The 64-m antennas are presently equipped with an electronic cam device which adjusts the hyperboloid's Z position with respect to the elevation angle. The curve is close to that given in Ref. 3 to maintain focus. The Y or lateral focussing is not available at present. However, when the pointing computer is upgraded, this function can be easily added.

(3) The match of the two curves on Fig. 5 should indicate the accuracy of the computed central pathlength changes.

(4) The pathlength changes are applicable only for the 64-m antenna at DSS 14. The overseas reflector structures are not alike until the "braces" described in Ref. 3 are attached.

(5) At the present time, there is available a second recording of the field focussed position (Ref. 5), which is different by about 0.25 cm at the extreme elevation angles from that of Ref. 2. These differences are not explainable at present, and may affect conclusion (3) above.

References

1. Katow, M. S., and Schmele, L. W., "Antenna Structures: Evaluation Techniques of Reflector Distortions," in *Supporting Research and Advanced Development, Space Programs Summary 37-40*, Vol. IV, pp. 176-184, Jet Propulsion Laboratory, Pasadena, Calif., Aug. 31, 1965.

2. Freiley, A. J., "Radio Frequency Performance of DSS 14 64-m Antenna at 3.56 and 1.96-cm Wavelength," Technical Report 32-1526, Vol. XIX, p. 110, Jet Propulsion Laboratory, Pasadena, Calif., Feb. 15, 1974.

3. Lobb, V. B., and Katow, M. S., "64-Meter-Diameter Antenna with New Braces: Installation Description and Computed Performance for Gravity Loads," Technical Report 32-1526, Vol. XVII, pp. 93-99, Jet Propulsion Laboratory, Pasadena, Calif., Oct. 15, 1973.

4. Katow, M. S., and Bartos, K. P., "Tricone Multiple Cassegrain Feed System for the 210-ft Antenna," in *Space Programs Summary 37-56*, Vol. II, pp. 121-124, Jet Propulsion Laboratory, Pasadena, Calif., Mar. 31, 1969.

5. Freiley, A. J., "Radio Frequency Performance of DSS 14 64-m Antenna at X-Band Using a Dual Hybrid Mode Feed," *DSN Progress Report 42-53, July and August 1979*, pp. 132-140, Jet Propulsion Laboratory, Pasadena, Calif.

Table 1. Best fit paraboloid data — gravity loading

Elevation angle, deg	Best-fit paraboloid data						
	Vertex		Focal length, m	Axis rotation, rad	Focus displacement		Best-fit rms mm
	Y-cm	Z-cm			Y-cm	Z-cm	
	(d′)	(d)	(e)	(f)	(g)	(h)	
10	5.089	0.191	27.09639	0.001132	2.023	−1.099	0.47
25	3.656	0.103	27.10246	0.000810	1.460	−0.580	0.26
35	2.059	0.048	27.10609	0.000455	0.827	−0.270	0.13
45	0	0	27.10927	0	0	0	0
55	−2.455	−0.041	27.11189	−0.000541	−0.987	0.221	0.12
65	−5.233	−0.074	27.11387	−0.001153	−2.106	0.384	0.24
80	−9.817	−0.104	27.11552	−0.002160	−4.214	0.514	0.39

$g = c - (f \times e)$

$h = d' + (e \times \cos f) - 27.10927$

Table 2. Hyperboloid axis displacements — gravity loading

Elevation angle, deg	RF feed phase center		Hyperbolid				Rotations	
			Vertex		Node 2094	Secondary focus change	Axis	Path
	Y-cm (m)	Z-cm (n)	Y-cm (i)	Z-cm (j)	Y-cm (ii)	Z-cm (v)	rad (p)	rad (o)
10	−0.667	0.221	−1.461	0.513	−1.420	0.081	0.000370	−0.000697
25	−0.472	0.183	−1.039	0.272	−1.008	0.043	0.000281	−0.000499
35	−0.263	0.057	−0.583	0.127	−0.564	0.020	0.000164	−0.000280
45	0	0	0	0	0	0	0	0
55	0.311	0.049	0.690	−0.105	0.667	−0.018	−0.000203	0.000333
65	0.659	0.089	1.466	−0.185	1.418	−0.031	−0.000436	0.000709
90	1.230	0.130	2.741	−0.252	2.648	−0.043	−0.000837	0.001328

$p = (ii–i) \times 111.35$

$o = (i–m)/(1137.993 + j–n)$

Table 3. Hyperboloid phase centers offsets – gravity loading

Elevation angle, deg	Ray incidence angle, rad (q)	Y offsets				Z offsets	
		cm (r)	cm (s)	cm (t)	cm (u)	cm (w)	cm (x)
10	0.001067	1.215	0.086	0.249	−1.126	0.592	−1.693
25	0.000780	0.888	0.066	0.182	−0.791	0.315	−0.895
35	0.000444	0.505	0.038	0.104	−0.441	0.147	−0.417
45	0	0	0	0	0	0	0
55	−0.000536	−0.610	−0.047	−0.125	0.518	−0.123	0.344
65	−0.001145	−1.303	−0.102	−0.268	1.096	−0.216	0.600
80	−0.002165	−2.463	−2.463	−0.506	2.039	−0.295	0.809

$r = q \times (a + j \text{ (Table 2)} + n \text{ (Table 2)})$

$s = p \times (b + v \text{ (Table 2)})$

$t = q \times (b + v \text{ (Table 2)})$

$u = i \text{ (Table 2)} - (s + t)$

$w = j \text{ (Table 2)} + v \text{ (Table 2)}$

$x = h \text{ (Table 1)} - w$

Table 4. RF pathlength changes with no Z focussing

Elevation angle, deg	Hyperboloid vertex Z displacement cm (j)	Primary RF feed Z displacement cm (n)	Best-fit vertex offset cm (d)	Pathlength change cm (aa)
10	0.513	0.221	0.191	0.42
25	0.272	0.120	0.103	0.22
35	0.127	0.057	0.048	0.10
45	0	0	0	0
55	−0.105	−0.049	−0.041	−0.08
65	−0.185	−0.089	−0.074	−0.13
80	−0.252	−0.130	−0.104	−0.17

$aa = (2 \ast j) - n - 2d$

Table 5. RF pathlength changes with Z axial focussing

Elevation angle, deg	Displacement at focus Z cm (h)	Primary RF feed displacement cm (n)	Best-fit vertex offset cm (d)	Pathlength change cm (aa)
10	−1.099	0.221	0.191	−2.80
25	−0.580	0.120	0.103	−1.49
35	−0.270	0.057	0.048	−0.69
45	0	0	0	0
55	0.221	−0.049	−0.041	0.57
65	0.384	−0.089	−0.074	1.01
80	0.514	−0.130	−0.104	1.37

Table 6. Field data to foci offset data

| Elevation angle, deg | Indicated control room position cm * | Adjust to 0 at 45° cm (A) | Jackscrews Z displacement | | | | Sum A + B + C cm (D) | Hyperboloid virtual focus correction cm (E) | Z foci offset D + E cm |
			Node 2182 cm	Node 2185 cm	Weighted average cm (B)	Bending displacement cm (C)			
10	−2.57	−2.11	0.041	0.493	0.460	0.081	−1.567	−0.079	−1.65
25	−1.52	−1.06	0.206	0.267	0.241	0.043	−0.782	−0.041	−0.82
35	−0.97	−0.51	0.091	0.127	0.112	0.020	−0.376	−0.020	−0.40
45	−0.46	0	0	0	0	0	0	0	0
55	−0.08	0.38	−0.066	−0.109	−0.091	−0.018	0.272	0.015	0.29
65	0.23	0.69	−0.102	−0.196	−0.158	−0.031	0.498	0.028	0.53
80	0.51	0.97	−0.102	−0.285	−0.211	−0.043	0.711	0.038	0.75

*May 1973 data (Ref. 2) for mechanism description (Ref. 4)

Table 7. Foci offsets gain loss — X band (8.45 GHz)

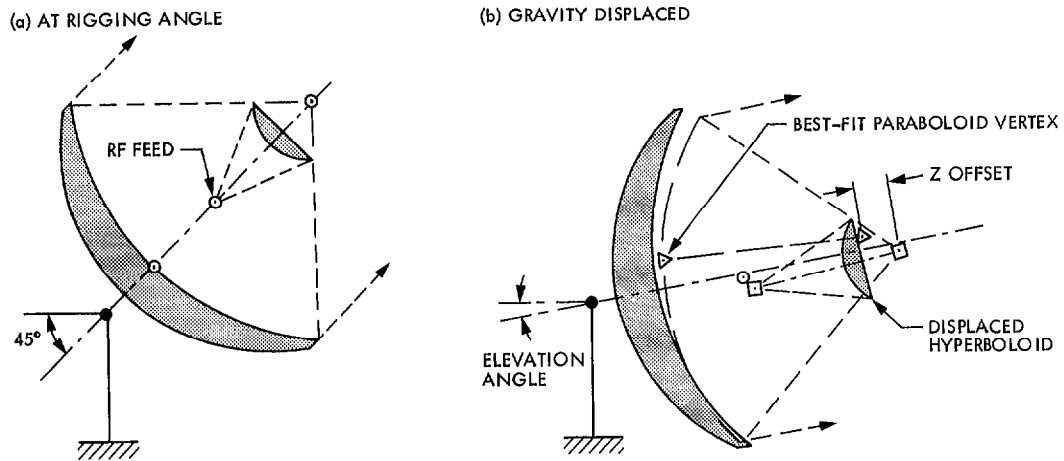| Elevation angle, deg | Foci offset | | Gain loss | |
	Y-cm (bb)	Z-cm (cc)	Y-dB, db	Z-dB, db
10	3.147	−1.694	0.13	0.79
25	2.250	−0.894	0.07	0.22
35	1.265	−0.416	0.02	0.05
45	0	0	0	0
55	−1.303	0.343	0.02	0.03
65	−3.205	0.599	0.13	0.09
80	−6.253	0.810	0.51	0.18

$bb = g + u$
$cc = h + j + v$

Fig. 1. 64-m antenna — RF optics

- ● UNDEFORMED OR RIGGED POINTS
- ✦ STRUCTURAL VERTEX
- △ BEST FIT PARABOLOID VERTEX
- ▣ HYPERBOLOID SYSTEM VIRTUAL FOCUS
- ◇ RF FEED PHASE CENTER
- ◔ BEST FIT PARABOLOID FOCUS
- ✕ HYPERBOLOID DESIGN FOCI
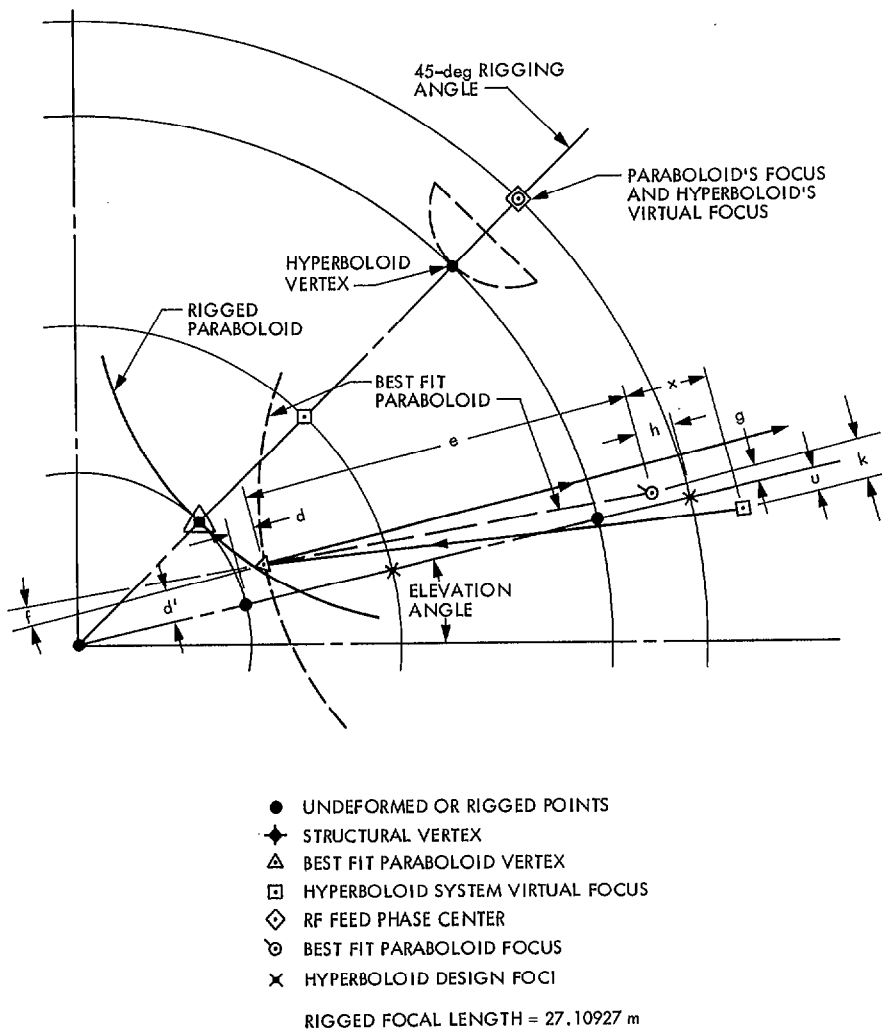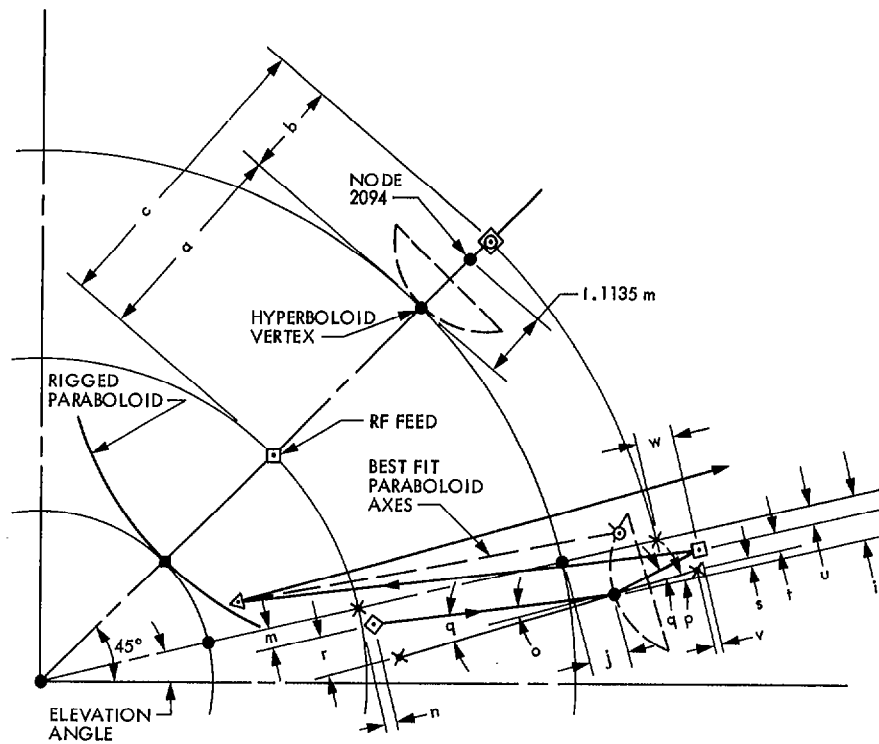
RIGGED FOCAL LENGTH = 27.10927 m

Fig. 2. Best fit paraboloid displacements — gravity loading

- ● UNDEFORMED OR RIGGED POINTS
- ✦ STRUCTURAL VERTEX
- △ BEST FIT PARABOLOID VERTEX
- ⊡ HYPERBOLOID SYSTEM VIRTUAL FOCUS
- ◇ RF FEED PHASE CENTER
- ⟁ BEST FIT PARABOLOID FOCUS
- ✗ HYPERBOLOID DESIGN FOCI

HYPERBOLOID DATA

a = 11.37993 m

b = 2.33607 m

c = 13.7160 m

Fig. 3. Hyperboloid system displacements – gravity loading

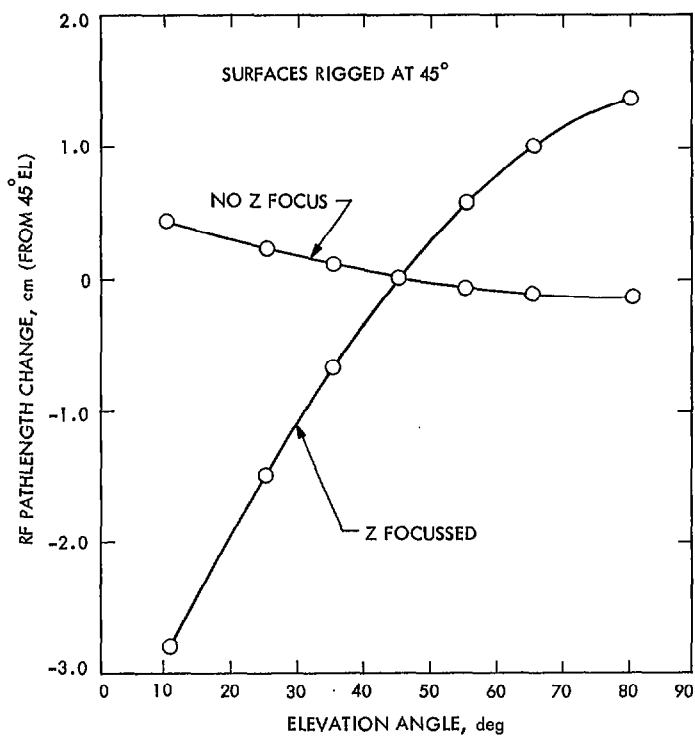**Fig. 4. RF pathlength changes vs elevation angle**

SURFACES RIGGED AT 45°

NO Z FOCUS

Z FOCUSSED

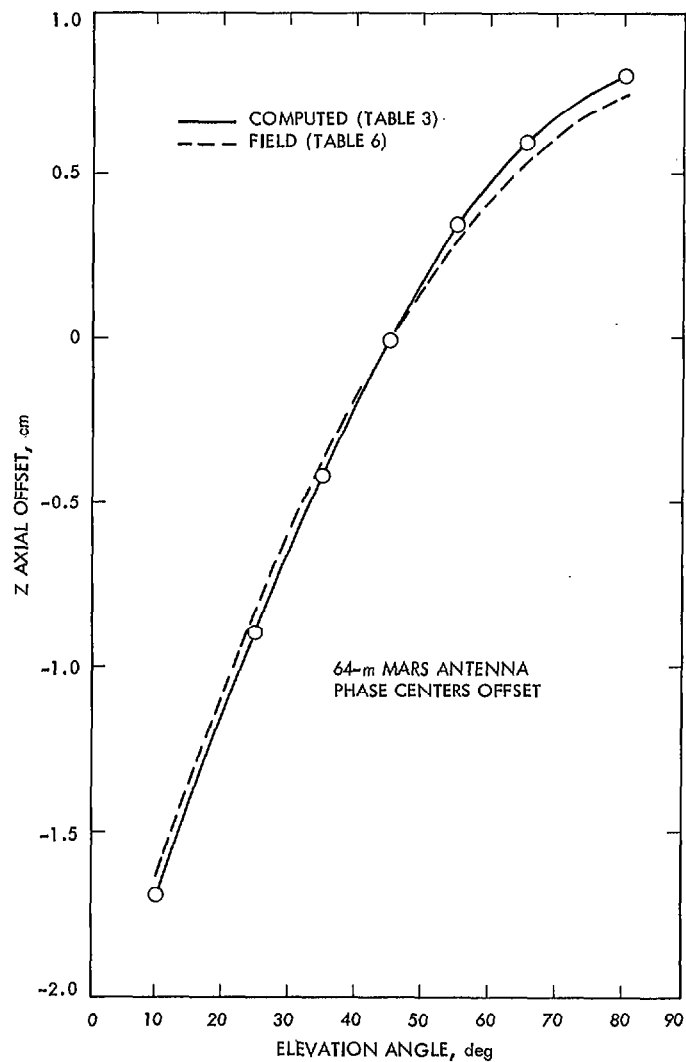COMPUTED (TABLE 3)

FIELD (TABLE 6)

64-m MARS ANTENNA
PHASE CENTERS OFFSET

Fig. 5. 64-m phase centers offset — computed vs field